# TRANSNUCLEAR, INC.

March 20, 2002                                                       E-19419

Mr. Steven Baggett, Senior Project Manager
Spent Fuel Project Office
Division of Industrial and Medical Nuclear Safety
Office of Nuclear Material Safety and Safeguards
Nuclear Regulatory Commission
11555 Rockville Pike
Rockville, MD 20852

Subject:     Docket No. 71-9302 (TAC No. L23328), Additional Clarification for the
             NUHOMS®-MP197 Transport Package Application dated October 24, 2001


Dear Mr. Baggett:

Enclosed for your review is additional clarification to our RAI response submittal on January 31,
2002. They consist of the following attachments:

a.     Revised SAR pages, Chapter 6 (whole chapter), Clarification for MP-197 RAI #1
       Response 6-6 (8 copies)
b.     Revised SAR drawing. Drawing No. 1093-71-15 (8 copies)

If you have any questions or comments, please call me.

Sincerely,

Peter Shih
Project Manager

cc:    1093 File
       Jayant Bondre – TNW
       Laruent Michels - TNP

NMSS01 Public

# NUHOMS®-MP197 TRANSPORT PACKAGING

## CHAPTER 6

## TABLE OF CONTENTS

CHAPTER 6

CRITICALITY EVALUATION

## 6.1    Design

The design criteria for the NUHOMS®-61BT Dry Shielded Canister (DSC) to be transported in the NUHOMS®-MP197 transport package require that the package remain subcritical under normal conditions of transport (NCT) and hypothetical accident conditions (HAC) as defined in 10CFR Part 71.

The NUHOMS®-61BT System's criticality safety is ensured by both fixed neutron absorbers and favorable geometry. Burnup credit is not taken in this criticality evaluation. The fixed neutron absorber may be one of several different types of borated metallic plates. The materials description, acceptance testing, and the boron 10 credit allowed for the various fixed absorber materials are included in Chapter 8.

No credit is taken for moderator exclusion by the DSC.

### 6.1.1    Discussion and Results

Figure 6-1 shows the cross section of the NUHOMS®-61BT DSC. The analysis presented herein is performed for a NUHOMS®-61BT DSC in a the MP-197 transportation cask. The cask consists of an inner stainless steel shell, and lead gamma shield, a stainless steel structural shell and a hydrogenous neutron shield. The NUHOMS®-MP197 configuration is shown to be subcritical under NCT and HAC.

The calculations determine $k_{eff}$ with the CSAS25 control module of SCALE-4.4 [6.1] for various configurations and initial enrichments, including all uncertainties to assure criticality safety under all credible conditions.

The results of the evaluation demonstrate that the maximum $k_{eff}$ - including statistical uncertainty - is less than the Upper Subcritical Limit (USL) determined from a statistical analysis of benchmark criticality experiments. The statistical analysis procedure includes a confidence band with an administrative safety margin of 0.05.

## 6.2    Package Fuel Loading

The NUHOMS®-MP-197 is capable of transporting intact BWR fuel assemblies with or without fuel channels. The maximum lattice-averaged enrichment of the fuel depends on the boron content in the fixed poison plates in the basket, as shown in Table 6-1. The fuel assemblies considered as authorized contents are listed in Table 6-2.

Table 6-3 lists the fuel parameters for the standard BWR fuel assemblies. The design basis fuel chosen for the NUHOMS®-MP197 Packaging criticality analysis is the GE 10×10 fuel assembly because it is the most reactive fuel assembly of the authorized contents, as demonstrated in the appendix to this chapter.

An infinite array of packages with optimal internal and interspersed moderation is evaluated to demonstrate compliance with 10CFR71.59(a)(1) and 10CFR71.59(a)(2). For 10CFR71.55(b), the effect of external reflection for a single cask is evaluated by modeling the confinement boundary (canister) surrounded by full density water. The variation in external reflection is provided by progressively modeling the various cask shells surrounding the canister, in separate calculations, surrounded by full density water. Because an infinite array of packages is used to evaluate both NCT and HAC, the transport index for criticality safety is zero.

## 6.3   Model Specification

The following subsections describe the physical models and materials of the NUHOMS®-MP197 packaging used for input to the CSAS25 module of SCALE-4.4 [6.1] to perform the criticality evaluation.

### 6.3.1   Description of Calculational Model

The cask and the DSC were explicitly modeled using the appropriate geometry options in KENO V.a of the CSAS25 module in SCALE-4.4.

Two models were developed.  The first model is a full-active fuel height model and full-radial cross section of the DSC alone with water boundary conditions on the ends and reflective boundary conditions on the sides.  The model does not include the gaps between the poison plates.  This model is more fully described in Section 6.6.2.  This model is only used to determine the most reactive fuel assembly/channel combination and to justify use of the lattice average enrichment for the intact fuel analysis.  The second model is a full-active fuel height model and full radial cross section of the cask and DSC with reflective boundary conditions on all sides.  This model includes the worst case gaps between the poison plates and the basket internals modeled at minimum material conditions.  This model includes the GE12 10×10-fuel assembly only because this assembly type is determined to be the most reactive fuel assembly type of the authorized contents.  The GE12 10×10-fuel assembly is modeled as a 10×10 array comprising 92 fuel rods, including fuel, gap and cladding and two large water holes.  The fuel cladding OD is also reduced by 0.010 inches in the final models to conservatively bound fuel manufacturing tolerances.

Figure 6-2 is a sketch of each KENO V.a unit showing all materials and dimensions for each unit and an annotated cross section map showing the assembled geometry units in the radial direction of the model. The assembly-to-assembly pitch is a variable in the model with the fuel assemblies modeled in the center of the fuel cells and pushed towards the center and away from the center of the basket.  The poison plates are modeled with

minimum plate thickness, width and length. The maximum gap between the plates is modeled in the worst case orientation to maximize the amount of "uncovered" fuel. The gaps between the poison plates are due to the need to provide space for thermal expansion of the poison plates relative to the stainless steel parts of the basket and to allow for fabrication tolerances in the basket. In addition, the NUHOMS®-61BT DSC design allows the poison plates to be fabricated in sections, rather than one continuous piece. In the axial direction, all gaps are modeled at the maximum width. Table 6-4 provides the axial position of the assembled KENO V.a geometry units. Figure 6-3 shows the second model in the bounding configuration.

An infinite array of damaged packages in a rectangular lattice is modeled by the use of mirror reflection on all six sides of a cuboid surrounding the package model (the second model described above). Neither the neutron shield nor the impact limiters are modeled, which reduces the pitch between packages in the array.

### 6.3.2 Package Regional Densities

The Oak Ridge National Laboratory (ORNL) SCALE code package [6.1] contains a standard material data library for common elements, compounds, and mixtures. All the materials used for the cask and DSC analysis are available in this data library. The neutron shield material in the MP197 is modeled as water and the neutron shield skin is not modeled.

Table 6-5 provides a complete list of all the relevant materials used for the criticality evaluation. The B-10 areal density specified for manufacturing of the poison plates will be larger than the areal density used in the calculations (and listed in this table), in order the satisfy the 75% or 90% B10 credit allowance as specified in Chapter 8. The cask neutron shield material is conservatively modeled as water. The actual neutron shield hydrogen atom density is lower than that of water; therefore, replacing the neutron shield with water is slightly conservative.

### 6.4 Criticality Calculation

This section describes the models used for the criticality analysis. The analyses were performed with the CSAS25 module of the SCALE system. A series of calculations were performed to determine the most reactive fuel and configuration. The most reactive fuel, as demonstrated by the analyses, is the GE12 10×10 assembly. The most reactive credible configuration is an infinite array of flooded casks with minimum assembly-to-assembly pitch and the poison plate gaps located near the center of the basket and at the centerline of the active fuel region.

## 6.4.1  Calculational Method

### 6.4.1.1 Computer Codes

The CSAS25 control module of SCALE-4.4 [6.1] was used to calculate the effective multiplication factor ($k_{eff}$) of the fuel in the cask. The CSAS25 control module allows simplified data input to the functional modules BONAMI-S, NITAWL-S, and KENO V.a. These modules process the required cross sections and calculate the $k_{eff}$ of the system. BONAMI-S performs resonance self-shielding calculations for nuclides that have Bondarenko data associated with their cross sections. NITAWL-S applies a Nordheim resonance self-shielding correction to nuclides having resonance parameters. Finally, KENO V.a calculates the $k_{eff}$ of a three-dimensional system. A sufficiently large number of neutron histories are run so that the standard deviation is below 0.0020 for all calculations.

### 6.4.1.2 Physical and Nuclear Data

The physical and nuclear data required for the criticality analysis include the fuel assembly data and cross-section data as described below.

The criticality analysis used the 44-group cross-section library built into the SCALE system. ORNL used ENDF/B-V data to develop this broad-group library specifically for criticality analysis of a wide variety of thermal systems.

### 6.4.1.3 Bases and Assumptions

The analytical results reported in chapter 2 demonstrate that the cask containment boundary and DSC basket structure do not experience any significant distortion under hypothetical accident conditions. Therefore, for both normal and hypothetical accident conditions the cask geometry is identical except for the neutron shield and skin. As discussed above, the neutron shield and skin are conservatively modeled as water.

The cask was modeled with KENO V.a using the available geometry input. This option allows a model to be constructed that uses regular geometric shapes to define the material boundaries. The following conservative assumptions were also incorporated into the criticality calculations:

1. Omission of grid plates, spacers, and hardware in the fuel assembly.

2. No burnable poisons accounted for in the fuel.

3. Water density at optimum internal and external moderator density.

4. Unirradiated fuel – no credit taken for fissile depletion due to burnup or fission product poisoning.

5. Where fuel pins have variable axial enrichment, the average is calculated for each axial zone (lattice), and the lattice with the highest average enrichment is used to characterize the entire bundle for criticality purposes. The average enrichment is defined as the simple arithmetic average of pin enrichments:

$$E_{avg} = \sum_{i=1,n} E_i \bigg/ n$$

Where $E_i$ is the enrichment of pin i, and n is the number of fuel pins in the lattice. There is no averaging of the axial enrichment variation in this evaluation; "bundle average" enrichments, which are an average enrichment over the entire fuel bundle, including natural uranium blankets, are not used to qualify fuel for criticality purposes.

The lattice average fuel enrichment is modeled as uniform everywhere throughout the assembly. Natural Uranium blankets and axial or radial enrichment zones are modeled as enriched uranium.

6. All fuel rods are assumed to be filled with 100% moderator in the pellet/cladding gap.

7. Only the active fuel length of each assembly type is explicitly modeled. The presence of the plenum materials, end fittings, channel material above and below the active fuel reduce the $k_{eff}$ of the system, therefore; these regions are modeled as water or the reflective boundary conditions. For the cases with reflective boundary conditions, the model is effectively infinitely long.

8. It is assumed that for all Hypothetical Accident Conditions (HAC) cases the neutron shield and stainless steel skin of the cask are stripped away and replaced with moderator.

9. The least material condition (LMC) is assumed for the fuel clad OD, fuel compartment, poison plates and wrappers. This minimizes neutron absorption in the steel sheets and poison plates.

10. The maximum allowed gap between the poison plates in the worst case position is explicitly modeled to maximize $k_{eff}$.

11. The active fuel region is conservatively assumed to start level with the bottom of the poison plates.

12. Temperature at 20 °C (293 K).

13. Used 95% theoretical density for fuel although this assumption conservatively increases the total fuel content in the model.

### 6.4.1.4 Determination of $k_{eff}$.

The criticality calculations were performed with the CSAS25 control module in SCALE-4.4. The Monte Carlo calculations performed with CSAS25 (KENO V.a) used a flat neutron starting distribution. The total number of histories traced for each calculation was approximately 500,000. This number of histories was sufficient to converge the source and produce standard deviations of less than 0.2% in $k_{eff}$. The maximum $k_{eff}$ for the calculation was determined with the following formula:

$$k_{eff} = k_{KENO} + 2\sigma_{KENO}.$$

### 6.4.2    Fuel Loading Optimization

A.    Determination of the Most Reactive Fuel Lattice

All fuel lattices, with and without channels, listed in Table 6-3 are evaluated to determine the most reactive fuel assembly type. The lattices are analyzed with water in the fuel pellet cladding annulus and are centered in the fuel compartments. Each lattice is also analyzed with a 0.065, 0.080 and 0.120 inch thick channel to determine the most reactive configuration. The results show that the reactivity change due to the fuel channels is within the statistical uncertainty of the KENO V.a calculations. Finally, this model is used for three cases that demonstrate that the use of lattice average enrichment is conservative for intact fuel. One case each for the GE2 (7x7 Array), GE5 (8x8 Array) and the GE9 (8x8 Array). Figure 6-5 provides a lattice map of the three assemblies evaluated including the enrichment modeled for each fuel pin. The following results are extracted from Table 6-6.

Lattice Average Compared to Variable Enrichment Models

| Assembly Version | Lattice Average Case $k_{eff}$ | Explicit Variable Enrichment Case $k_{eff}$ |
|---|---|---|
| GE2 (7x7 Array) | 0.9061 | 0.8971 |
| GE5 (8x8 Array) | 0.9031 | 0.8973 |
| GE9 (8x8 Array) | 0.9069 | 0.9034 |

For this analysis, only the DSC is modeled. The DSC is modeled over the active fuel height of the fuel with water reflectors at the ends (z) and reflective boundary conditions outside the DSC (infinite array in the x-y directions) The DSC model for this evaluation differs from the actual design in the following ways:

- the boron 10 areal density specified for manufacturing the poison plates will be greater than that used in the model, as described in Chapter 8,
- no gaps between poison plates are modeled,
- the stainless steel basket rails, which hold the basket together, are modeled as water.

Rev. 2   3/18

In all other respects, the model is the same as that described in Sections 6.3.1 and 6.3.2. The sole purpose of this model is to determine the *relative* reactivity of different fuel lattices in a configuration similar to the actual DSC.

A typical input file is included in Section 6.6.3. The results of these calculations are listed in Table 6-6. The most reactive fuel lattice evaluated for the DSC design is the GE generation 12 lattice, 10×10 array, without a fuel channel.

B.    Determination of the Most Reactive Configuration

The fuel-loading configuration of the DSC/cask affects the reactivity of the package. Several series of analyses determined the most reactive configuration for the DSC/cask.

For this analysis, the DSC/cask is modeled. The DSC/cask is modeled over the active fuel height of the fuel with reflective boundary conditions on all sides of the model, this represents and infinite array in the x-y direction of DSC/casks that are infinite in length. The DSC/cask model for this evaluation differs from the actual design in the following ways:

- the boron 10 areal density specified for manufacturing the poison plates will be greater than that used in the model, as described in Chapter 8,
- maximum gaps between poison plates are modeled in their worst case configuration,
- the stainless steel basket rails, which hold the basket together, are modeled as water.

The models are fully described in Section 6.3.1. The purpose of these models is to determine the most reactive configuration for intact fuel assemblies. A typical input file is included in Section 6.6.3.

The first series of analyses determined the most reactive fuel assembly-to-assembly pitch. The maximum lattice average fuel enrichment (4.4 wt. % U-235) and a poison plate boron-10 areal density of 0.036 g/cm$^2$ are used in the model. The results in Table 6-7 show the most reactive configuration occurs with minimum assembly-to-assembly pitch. The model is similar to the model shown in Table 6-4 and Figure 6-2 except that the nominal fuel cell size, nominal poison sheet thickness, fuel clad OD are used and the assemblies are moved within the fuel compartment to vary the assembly-to-assembly pitch.

The second set of analysis evaluates the effect of canister shell thickness on the system reactivity. The model starts with the most reactive assembly-to-assembly pitch (minimum pitch) case above and the canister shell thickness is varied from 0.49 to 0.55 inches. As demonstrated by the results the variation of shell thickness within the tolerance range is statistically insignificant. The nominal shell thickness is used throughout the rest of the analysis except that one additional case is added for the most reactive canister configuration (minimum poison plate thickness and minimum fuel cell size) to demonstrate that the slightly higher result for the maximum shell thickness is indeed a result of the statistics of the calculation.

The third set of analysis evaluates the effect of poison plate thickness on the system reactivity. The model starts with the most reactive assembly-to-assembly pitch (minimum pitch) case above and the poison plate thickness is modeled at 0.3 inches (minimum). The poison plate B-10 volume density is increased from 0.046 to 0.04724 g B10/cm$^3$ to maintain the areal density of 36 mg B10/cm$^2$ for the reduced plate thickness. Based on the results of this evaluation the balance of the calculations will use the minimum poison plate thickness because it represents a more reactive condition.

The fourth set of analysis evaluates the sensitivity of the system reactivity on fuel cladding OD. The model starts with the minimum poison plate case above and the fuel cladding OD is varied from 0.404 to 0.394 inches. Based on the results of this analysis, it is conservative to model the GE12 10x10 assembly cladding as 0.010 inches less than that reported in Table 6-3 for the balance of this evaluation.

The fifth set of analysis evaluates the effect of fuel cell size on the system reactivity. The model starts with the most reactive fuel clad OD case above and the canister fuel cell width is varied from 5.8 to 6.1 inches. The results show that the most reactive configuration is with the minimum fuel cell size. One additional run is made to verify that the canister maximum shell thickness does not increase reactivity. The balance of this evaluation will use the minimum cell size because it represents the most reactive configuration.

The sixth set of analyses evaluates the effect of internal moderator density on reactivity. The model starts with the most fuel cell width (minimum fuel cell width) case above. The internal moderator is varied from 100 to 0 percent full density. The results in Table 6-7 confirm that the most reactive condition occurs at full internal moderator density.

The seventh set of analyses evaluates the effect of external moderator density on reactivity. The model uses the most reactive case with internal moderator (full density) density and the external internal moderator is varied from 100 to 0 percent full density. The results in Table 6-7 show that the system reactivity is not affected by external moderator density. The variation in the results is due entirely to the statistical uncertainties in Keno V.a. Nonetheless, the apparent maximum value of $k_{eff}$, which occurs at 70% external moderator density, is the value reported for the damaged package array.

Finally, minimum boron 10 areal density in the poison plate as a function of lattice average initial enrichment is evaluated. These models represent the most reactive intact fuel assembly (GE12, 10x10) with a minimum assembly-to-assembly pitch, nominal shell thickness, minimum poison plate thickness, minimum fuel clad OD, minimum fuel cell width with full internal and external moderator density. The initial lattice average fuel enrichment is varied as well as the boron-10 density in the poison plates. These cases are used to specify a minimum boron-10 areal density as a function of maximum lattice average assembly enrichment. The results are reported in Table 6-7.

## 6.4.3    Criticality Results (Infinite Array)

Table 6-8 lists the results that bound all normal and hypothetical accident conditions. These criticality calculations were performed with CSAS25 of SCALE-4.4. For each case, the result includes (1) the KENO-calculated $k_{KENO}$; (2) the one sigma uncertainty $\sigma_{KENO}$; and (3) the final $k_{eff}$, which is equal to $k_{KENO} + 2\sigma_{KENO}$. Table 6-8 lists the poison plate boron-10 areal density used in the calculations as a function of the initial lattice average enrichment for the fuel assemblies.

The criterion for subcriticality is that

$$k_{KENO} + 2\sigma_{KENO} < USL,$$

where USL is the upper subcritical limit established by an analysis of benchmark criticality experiments. From Section 6.5, the minimum USL over the parameter range (in this case, pitch) is 0.9414. From Table 6-8 for the most reactive case,

$$k_{KENO} + 2\sigma_{KENO} = 0.9365 + 2\,(0.0011) = 0.9387 < 0.9414.$$

## 6.4.4    Criticality Results (Single Cask)

The criticality evaluations for a single cask are shown in the following table. The single cask models KENO are based on the most reactive infinite array case shown in Table 6-8. Separate KENO models are generated based on progressively modeling the various cask shells around the canister. A total of four single cask models are analyzed based on water reflection after 1) canister, 2) inner steel shell, 3) lead shell and 4) outer steel shell.

### Single Cask Calculation Results

| Description | $K_{eff} \pm \sigma$ | $K_{eff} \pm 2\sigma$ |
|---|---|---|
| Most reactive infinite array case from Table 6-8 - Reference model (full density external moderator) | $0.9349 \pm 0.0011$ | 0.9371 |
| Single cask, based on Reference model, with water reflector around Canister | $0.9345 \pm 0.0012$ | 0.9369 |
| Single cask, based on Reference model, with water reflector around the inner steel shell of Cask | $0.9330 \pm 0.0012$ | 0.9354 |
| Single cask, based on Reference model, with water reflector around the lead shell of Cask | $0.9349 \pm 0.0011$ | 0.9371 |
| Single cask, based on Reference model, with water reflector around the outer steel shell of Cask | $0.9346 \pm 0.0011$ | 0.9368 |

The results of the criticality calculations based on indicate single cask models are bounded by the infinite array results.

Rev. 2   3/18

## 6.5 Critical Benchmark Experiments

The criticality safety analysis of the NUHOMS®-MP197 System used the CSAS25 module of the SCALE system of codes.

The analysis presented herein uses the fresh fuel assumption for criticality analysis. The analysis employed the 44-group ENDF/B-V cross-section library because it has a small bias, as determined by the 125 benchmark calculations described in reference [6.2]. The upper USL-1 was determined using the results of these 125 benchmark calculations.

The benchmark problems used to perform this verification are representative of benchmark arrays of commercial light water reactor (LWR) fuels with the following characteristics:

(1) water moderation

(2) boron neutron absorbers

(3) unirradiated light water reactor type fuel (no fission products or "burnup credit") near room temperature (vs. reactor operating temperature)

(4) close reflection

(5) Uranium Oxide

The 125 uranium oxide experiments were chosen to model a wide range of uranium enrichments, fuel pin pitches, assembly separation, concentration of soluble boron and control elements in order to test the codes ability to accurately calculate $k_{eff}$. These experiments are discussed in detail in reference [6.2]. The file-input names referred to in the following sub-sections are identical to those used in [6.2].

### 6.5.1 Benchmark Experiments and Applicability

A summary of all of the pertinent parameters for each experiment is included in Table 6-9 along with the results of each run. The best correlation is observed for fuel assembly separation distance with a correlation of 0.65. All other parameters show much lower correlation ratios indicating no real correlation. All parameters were evaluated for trends and to determine the most conservative USL.

The USL is calculated in accordance to NUREG/CR-6361 [6.3]. USL Method 1 (USL-1) applies a statistical calculation of the bias and its uncertainty plus an administrative margin (0.05) to the linear fit of results of the experimental benchmark data. The basis for the administrative margin is from reference [6.4]. Results from the USL evaluation are presented in Table 6-10.

The criticality evaluation used the same cross section set, fuel materials and similar material/geometry options that were used in the 125 benchmark calculations as shown in Table 6-9. The modeling techniques and the applicable parameters listed in Table 6-11

for the actual criticality evaluations fall within the range of those addressed by the benchmarks in Table 6-9.

## 6.5.2    Results of the Benchmark Calculations

The results from the comparisons of physical parameters of each of the fuel assembly types to the applicable USL value are presented in Table 6-11. The minimum value of the USL was determined to be 0.9414 based on comparisons to the limiting assembly parameters as shown in Table 6-11.

Rev. 2    3/18
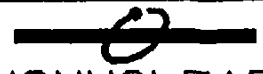
| 2 | 8/19/02 | SEE DCN 1093-84 | R.M. | P.S. | P.S. | M.M. | R.F. | P.S. |
| 1 | 1/25/02 | SEE DCN 1093-78 | R.M. | P.S. | P.S. | M.M. | R.F. | P.S. |
| NO. | DATE | REVISIONS | DWN. | CHK'D. | M.E. | N/T | Q/A | PROJ. |

| APPROVALS | DATE | | | |
|---|---|---|---|---|
| P.S. PROJ. | 1 MAY 01 | TRANSNUCLEAR, INC. HAWTHORNE, N.Y. | | |
| W.R.S. Q/A | 1 MAY 01 | NUHOMS®-61BT TRANSPORTABLE CANISTER | | |
| N/T | | FOR BWR FUEL | | |
| J.C. MECH. ENG. | 1 MAY 01 | SHELL ASSEMBLY | | SAR |
| P.S. CHK'D. BY | 1 MAY 01 | | | |
| J.T.G. DWN. BY | 27 APR. 01 | NONE SCALE | B SIZE | 1093-71-15 DWG. NO. | 2 REV. |